

SUPPLEMENTARY INFORMATION FOR

(R)-Profens Are Substrate-Selective Inhibitors of Endocannabinoid Oxygenation by COX-2

Kelsey C. Duggan^{†¶}, Daniel J. Hermanson^{†¶}, Joel Musee[†], Jeffery J. Prusakiewicz[†], Jami L. Scheib[†], Bruce D. Carter[†], Surajit Banerjee[‡], J.A. Oates[§], and Lawrence J. Marnett^{†*}

[†]A.B. Hancock Jr. Memorial Laboratory for Cancer Research, Departments of Biochemistry, Chemistry, and Pharmacology, Vanderbilt Institute of Chemical Biology, Center in Molecular Toxicology, and Vanderbilt-Ingram Cancer Center, [§]Division of Clinical Pharmacology and Department of Medicine, Vanderbilt University School of Medicine, Nashville TN 37232-0146

[‡]Northeastern Collaborative Access Team and Department of Chemistry and Chemical Biology, Cornell University, Building 436E, Argonne National Laboratory, 9700 S. Cass Avenue, Argonne, IL 60439

*To whom correspondence should be addressed

(p) 615-343-7329

(f) 615-343-7534

larry.marnett@vanderbilt.edu

[¶]These authors contributed equally to this work.

SUPPLEMENTARY METHODS

The supplementary methods are described in the legends to Figures 2, 8, 9, 10, and 11.

SUPPLEMENTARY RESULTS

Supplementary Tables

Supplementary Table 1 Data collection and refinement statistics for the (*R*)-naproxen-mCOX-2 and (*R*)-flurbiprofen-mCOX-2 complexes.

Data collection	(<i>R</i>)-naproxen	(<i>R</i>)-flurbiprofen
Space group	I222	P2 ₁ 2 ₁ 2
Cell dimensions a, b, c (Å) α, β, γ (°)	122.74, 133.03, 181.04 90.00, 90.00, 90.00	180.62, 134.55, 122.78 90.00, 90.00, 90.00
Resolution (Å)	2.4 (2.48-2.40)	2.85 (2.95-2.85)
R_{merge} (%)	11.7 (43.4)	11.8 (54.3)
I/σ	15.7 (3.6)	11.7 (3.3)
Completeness (%)	99.9 (100.0)	95.1 (92.2)
Redundancy	5.7 (5.8)	5.5 (5.3)
Refinement		
Resolution (Å)	2.4	2.85
No. reflections	55701	62160
$R_{\text{work}} / R_{\text{free}}$ (%)	17.7 / 23.3	19.7 / 24.4
No. of atoms		
Protein	8946	17896
Ligand / Ions	332 / 2	588 / 0
Water	601	241
B-factors		
Protein	28.6	47.8
Ligand / Ions	42.0 / 33.0	59.4 / 0
Water	31.7	37.9
Estimated Coordinate Error (Å)		
Luzzati plot	0.25	0.35
Maximum likelihood	0.29	0.36
R.m.s. deviations		
Bond lengths (Å)	0.008	0.009
Bond angles (°)	1.3	1.2

Values in parentheses correspond to the highest resolution shells.

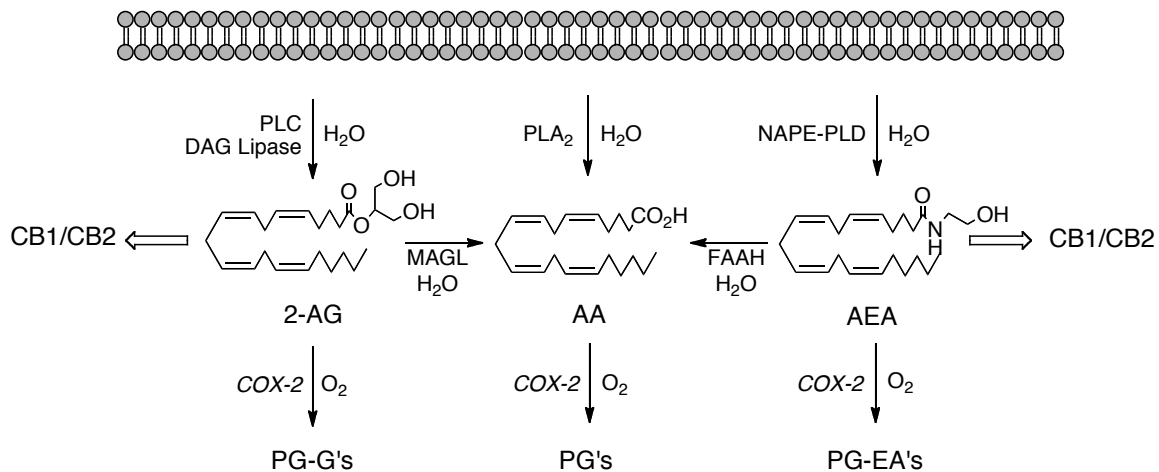
$R_{\text{merge}} = \frac{\sum_{hkl} \sum_{j=1, N} | \langle I_{hkl} \rangle - I_{hkj} |}{\sum_{hkl} \sum_{j=1, N} | I_{hkj} |}$ where the outer sum (*hkl*) is taken over the unique reflections.

$R_{\text{work}} = \frac{\sum_{hkl} ||F_{o,hkl} - k|F_{c,hkl}||}{\sum_{hkl} |F_{o,hkl}|}$, where $|F_{o,hkl}|$ and $|F_{c,hkl}|$ are the observed and calculated structure factor amplitudes, respectively.

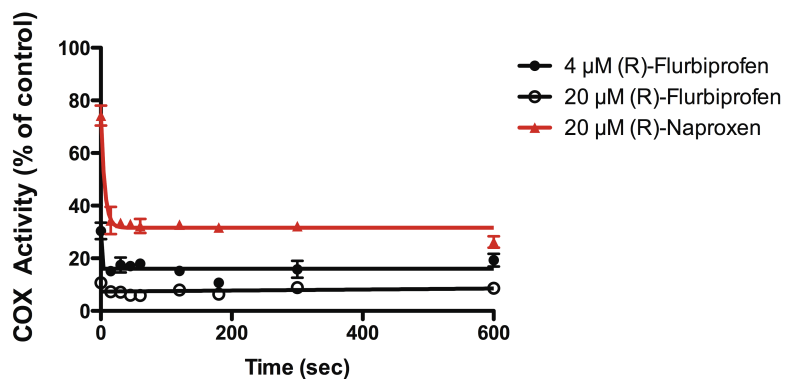
R_{free} is same as for R_{work} for the set of reflections (5% of the total) omitted from the refinement process.

NE-CAT, North Eastern Collaborative Access Team

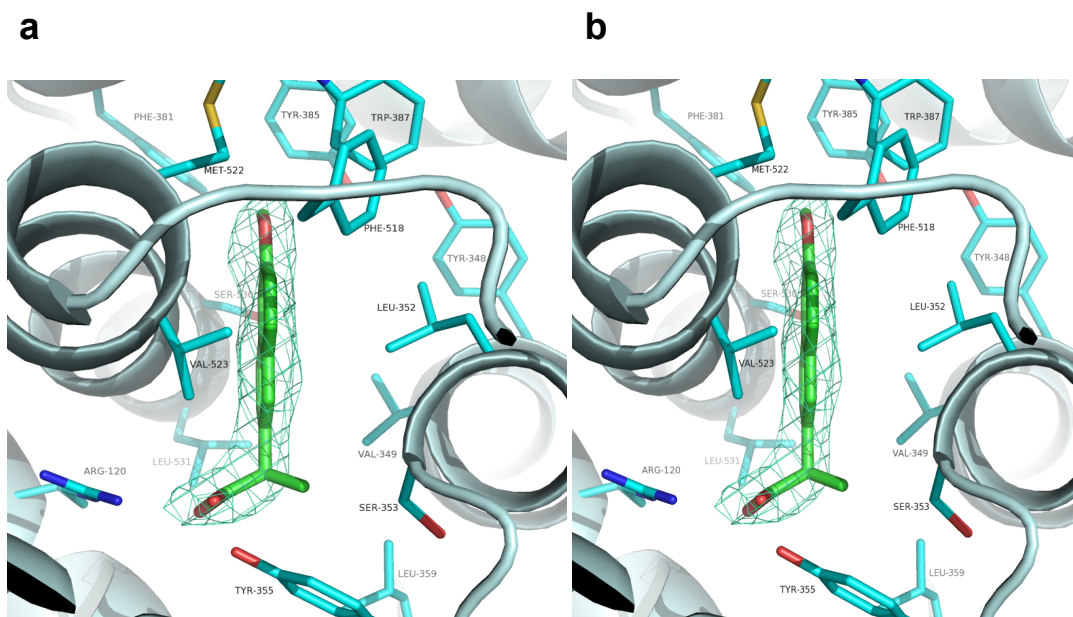
Supplementary Figures



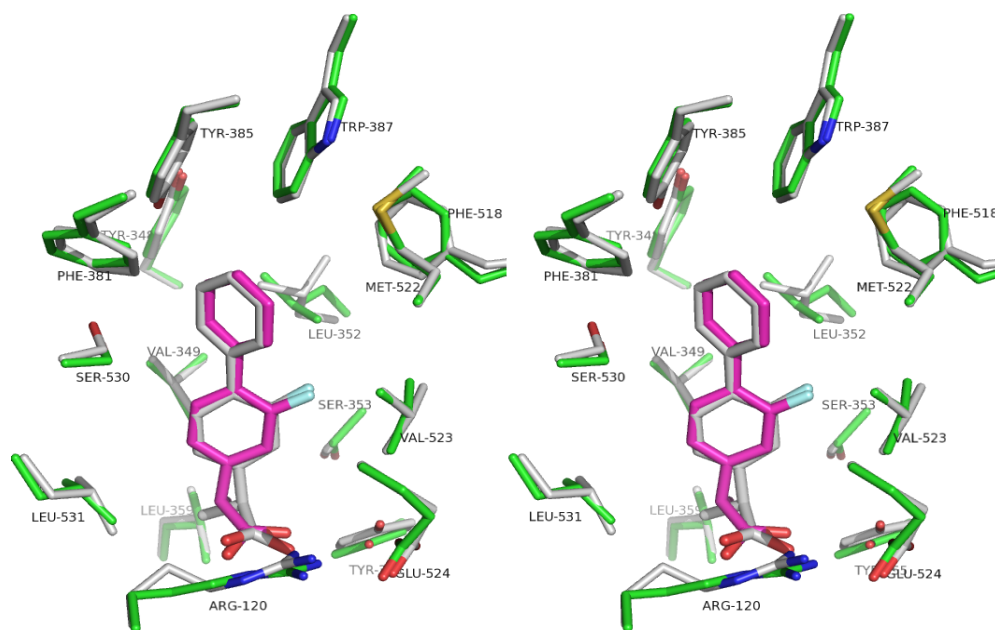
Supplementary Figure 1. Endocannabinoid metabolism. The pathways for the release of 2-AG, AA, and AEA, their oxygenation by COX-2 and the hydrolysis of 2-AG by MAGL and of AEA by FAAH are illustrated.



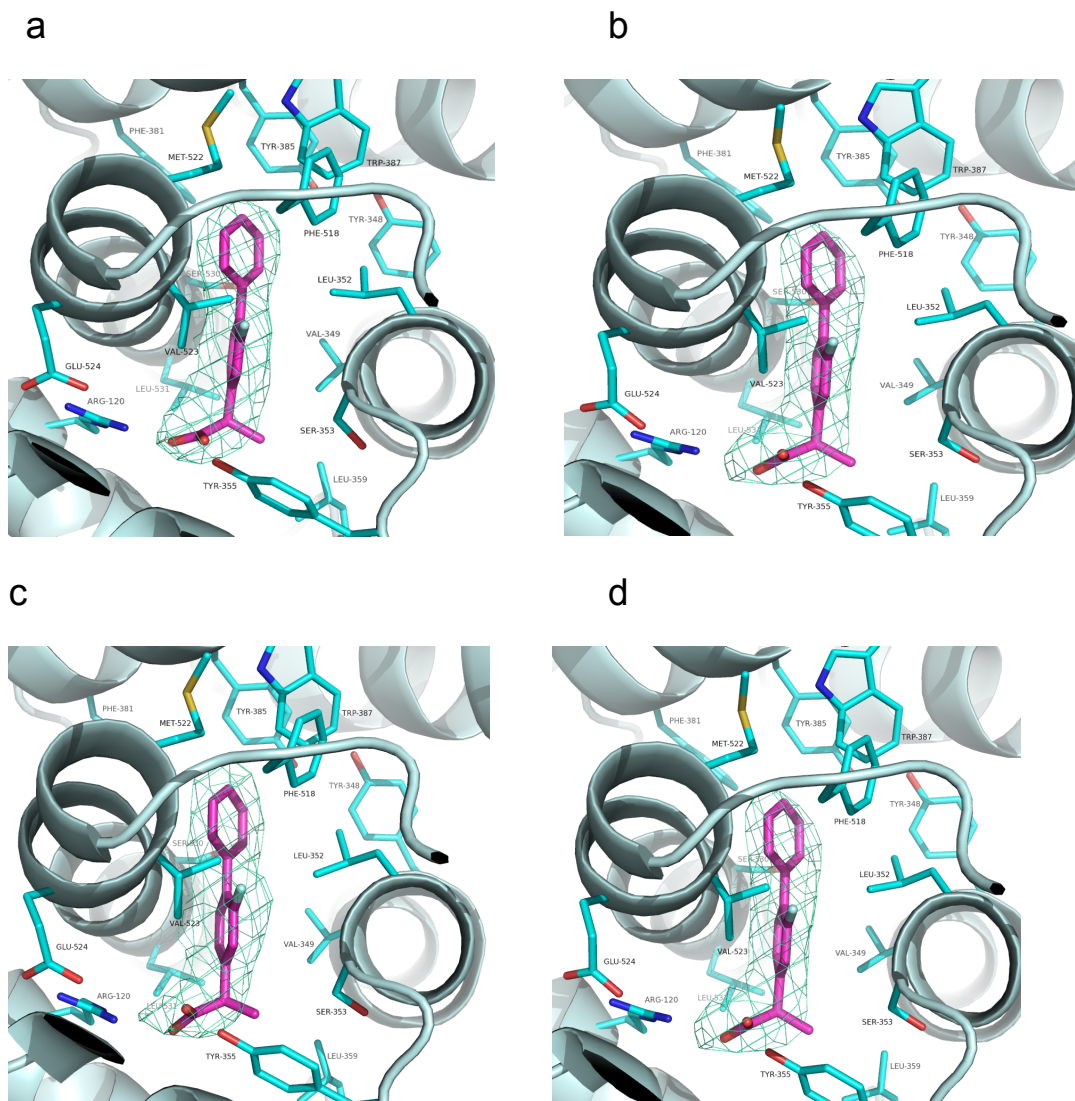
Supplementary Figure 2. Time-dependence of the inhibition of COX-2 mediated 2-AG metabolism by (*R*)-profens. (*R*)-flurbiprofen (4 or 20 μ M) or (*R*)-naproxen (20 μ M) were incubated with mCOX-2 for 0, 15, 30, 45, 60, 120, 180, 300 or 600 sec prior to the addition of a saturating concentration of 2-AG for 30 sec. Reactions were quenched and PG-G's were measured by LC-MS/MS as described under "Methods".



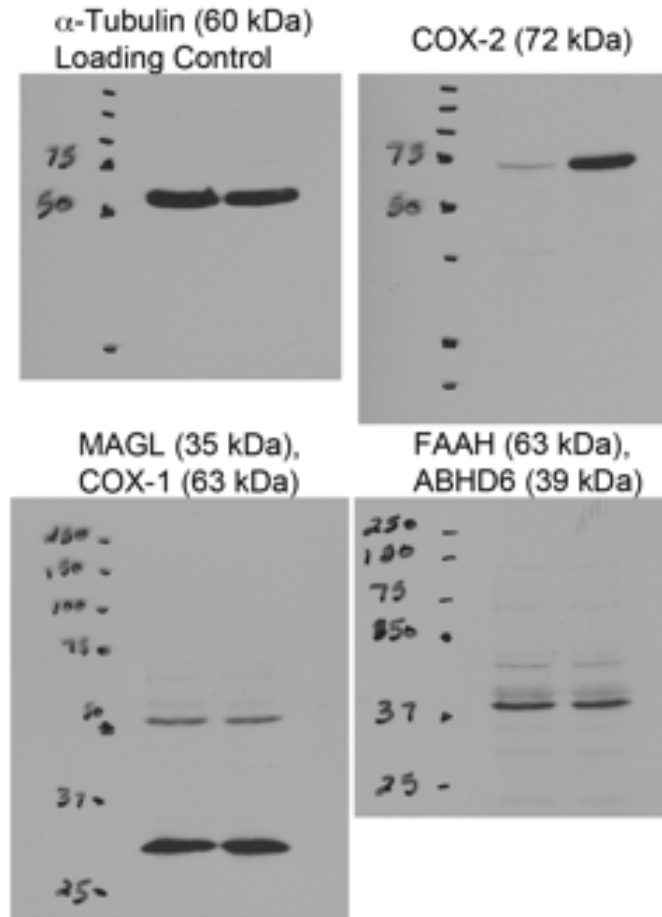
Supplementary Figure 3. Binding mode of (*R*)-naproxen within the active site of each of the COX-2 monomers comprising the homodimer. (a) represents “Monomer A” and (b) represents “Monomer B”. (*R*)-naproxen is shown in green sticks and surrounding protein residues are shown in cyan. The simulated annealing omit map (F_o-F_c) contoured at 3σ is shown surrounding the inhibitor.



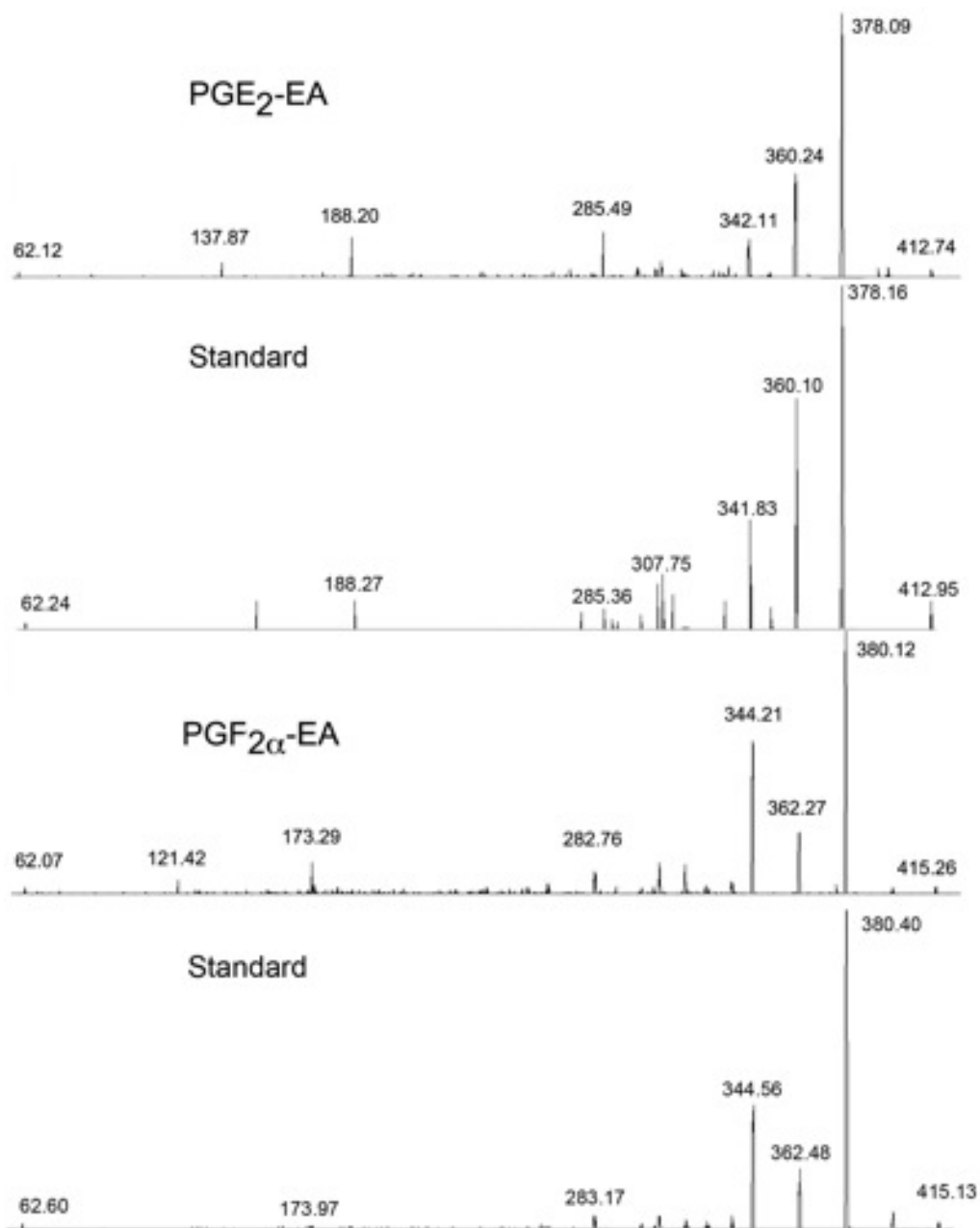
Supplementary Figure 4. Stereoview of the overlay of (*R*)- and (*S*)-flurbiprofen bound to mCOX-2. The crystal structure of the (*R*)-flurbiprofen-mCOX-2 complex is shown overlaid with the (*S*)-flurbiprofen-mCOX-2 complex reported by Kurumbail *et al.* (PDB ID: 3PGH) (ref). (*R*)-Flurbiprofen is shown in magenta with corresponding protein residues shown in green. The inhibitor and amino acid residues from the (*S*)-flurbiprofen-mCOX-2 structure are shown in grey.



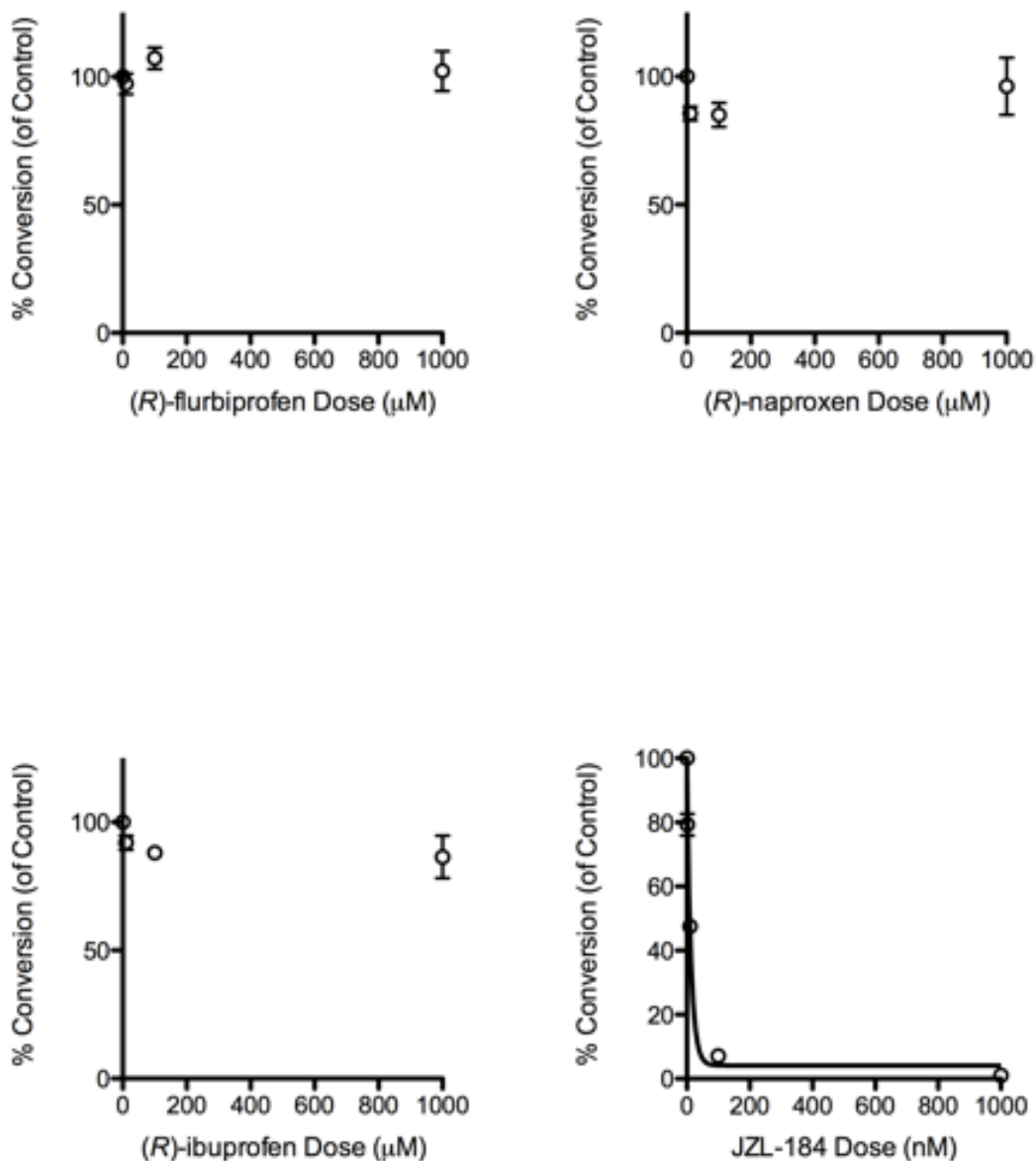
Supplementary Figure 5. *(R)*-flurbiprofen bound in the active site of each of the monomers in the crystallographic asymmetric unit. The inhibitor is shown in magenta with the surrounding simulated annealing omit map ($F_o - F_c$) displayed. The map is contoured at 3σ . Surrounding protein atoms are shown in cyan.



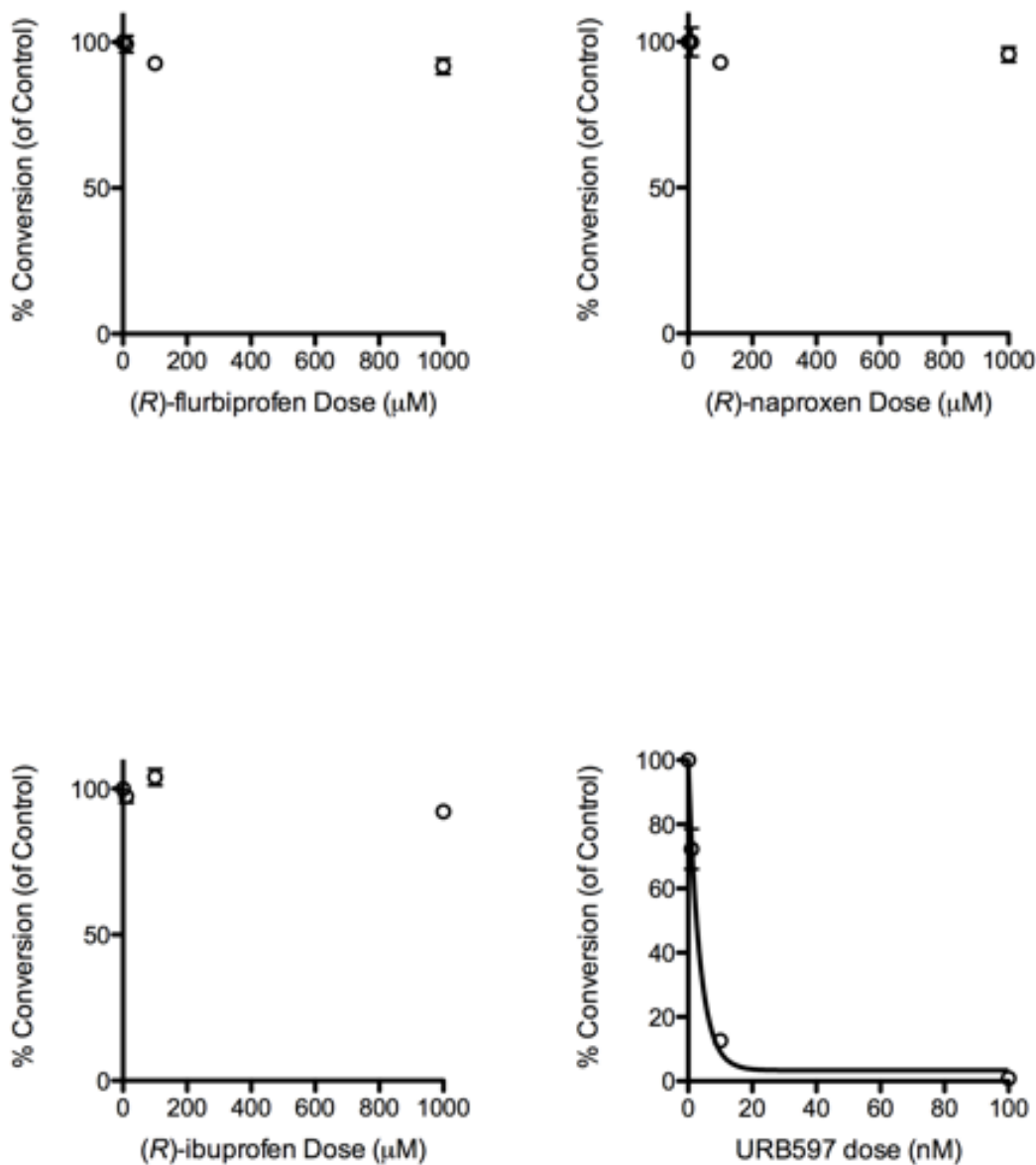
Supplementary Figure 6. Full, uncut Western blot analysis of basal (left lane) versus stimulated (right lane) DRG.



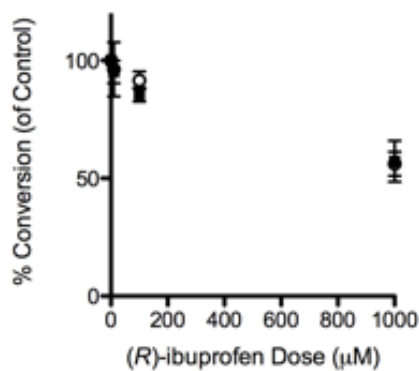
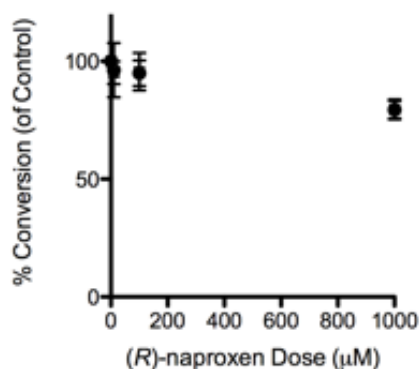
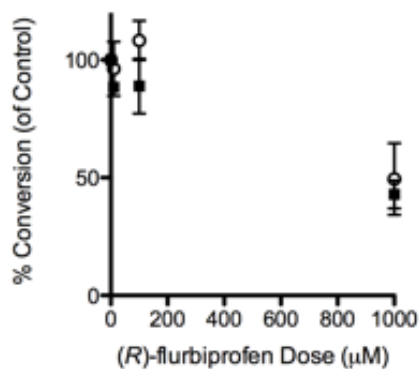
Supplementary Figure 7. Comparison of the MS/MS fragmentation patterns of the compounds eluting at the positions of PGF_{2α}-EA and PGE₂-EA isolated from DRGs to standards.



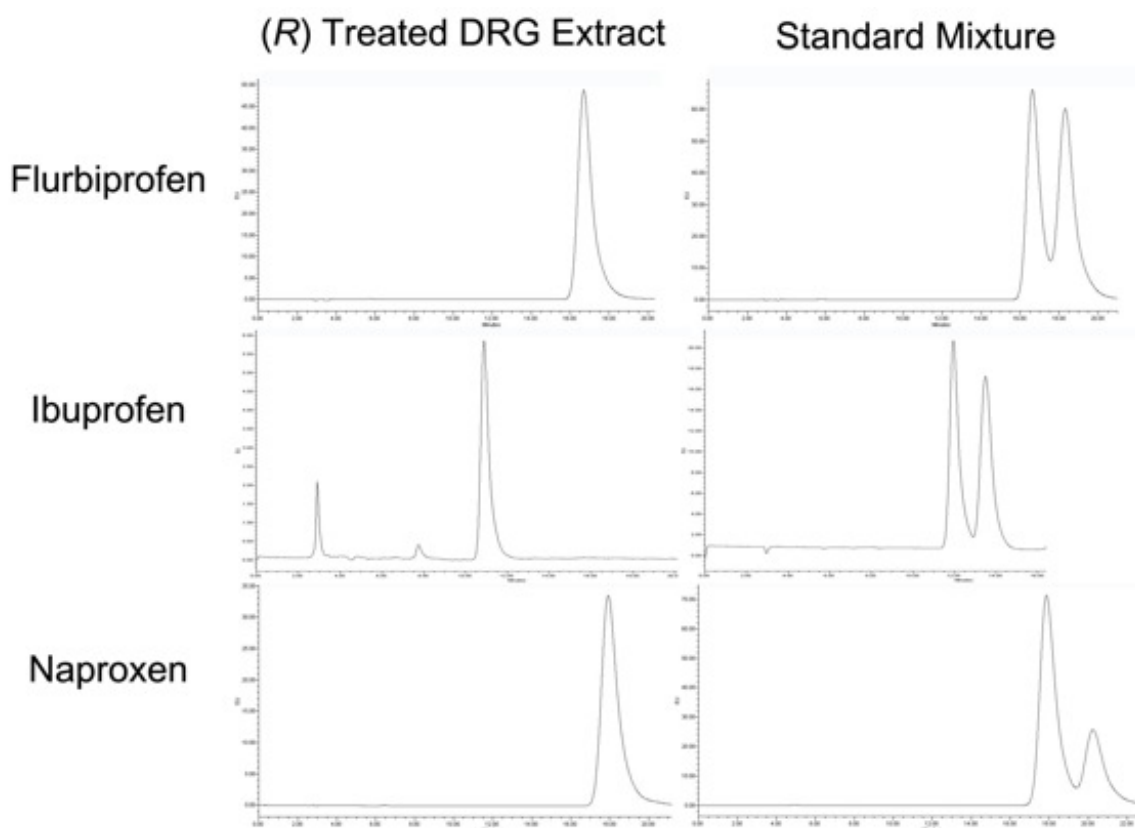
Supplementary Figure 8. Inhibition of human MAGL *in vitro* by (*R*)-flurbiprofen, (*R*)-naproxen, (*R*)-ibuprofen, and a known MAGL inhibitor, JZL 184. The compounds were pre-incubated with human recombinant MAGL for 5 minutes at 37°C before addition of 50 μM 2-AG for 5 minutes. The reactions were quenched and conversion of 2-AG to AA was quantified using SRM LC-MS-MS. Silver-associated fatty acid ions were monitored using the following transitions: 2-AG 485 \rightarrow 411, 2-AG-d8 493 \rightarrow 419, AA 519 \rightarrow 409, AA-d8 527 \rightarrow 417. Minimal inhibition of MAGL by (*R*)-profens was observed while the IC_{50} for JZL-184 was 9 nM.



Supplementary Figure 9. Inhibition of humanized rat FAAH by (*R*)-profens *in vitro*. The inhibition of FAAH by (*R*)-flurbiprofen, (*R*)-naproxen, and (*R*)-ibuprofen was measured and compared to FAAH inhibition by URB 597, a known FAAH inhibitor. The inhibitors were pre-incubated with humanized rat FAAH for 5 minutes at 37°C prior to the addition of 50 μM AEA. The reaction was quenched after 5 minutes, and conversion of AEA to AA was quantified by SRM LC-MS/MS. The levels of AEA and AA were monitored using the following transitions: AEA 456 \rightarrow 438, AEA-d8 464 \rightarrow 446, AA 519 \rightarrow 409, and AA-d8 527 \rightarrow 417 for silver-associated ions. The IC_{50} value for URB597 was determined to be 2 nM but no inhibition of FAAH by (*R*)-profens was observed at concentrations up to 1 mM.



Supplementary Figure 10. Inhibition of human 15-lipoxygenase-1 by (*R*)-flurbiprofen, (*R*)-naproxen, and (*R*)-ibuprofen *in vitro*. The extent of inhibition was assessed by pre-incubating the inhibitors with enzyme for 5 minutes at 37°C followed by the addition of 50 µM of either AA or 2-AG for 30 seconds. The reactions were then quenched and conversion of AA or 2-AG to 15-HETE (■) or 15-HETE-G (○) was detected and quantified using HPLC and UV absorbance at 236 nm. The 15-HETE and 15-HETE-G were distinguished based on retention time and a standard curve was used to quantify the peak areas.



Supplementary Figure 11. Analysis of (*R*)-flurbiprofen, (*R*)-naproxen, and (*R*)-ibuprofen treated DRG extracts using chiral HPLC and fluorescence. A Daicel chiralpak chiral column was used in conjunction with a normal-phase HPLC gradient to separate the profen enantiomers. Conversion of (*R*)-flurbiprofen, (*R*)-naproxen, and (*R*)-ibuprofen to (*S*)-flurbiprofen, (*S*)-naproxen, and (*S*)-ibuprofen does not occur over the time course used in the experiment. An analysis of standard mixtures of flurbiprofen, naproxen, and ibuprofen enantiomers shows the chromatography and separation of the two enantiomers.